

# UC San Diego

## UC San Diego Previously Published Works

### Title

Native paraneurial tissue and paraneurial adhesions alter nerve strain distribution in rat sciatic nerves

### Permalink

<https://escholarship.org/uc/item/3h11n3gm>

### Journal

Journal of Hand Surgery (European Volume), 43(3)

### ISSN

1753-1934

### Authors

Foran, Ian M  
Hussey, Vincent  
Patel, Rushil A  
[et al.](#)

### Publication Date

2018-03-01

### DOI

10.1177/1753193417734433

Peer reviewed

1 **Native paraneurial tissue and paraneurial adhesions alter nerve strain distribution**  
2 **in rat sciatic nerves**

3 Ian M. Foran, MD<sup>1</sup>, Vincent Hussey, MS<sup>1</sup>, Rushil A. Patel<sup>1</sup>,

4 Jaemyoung Sung<sup>1</sup>, Sameer B. Shah, PhD<sup>1,2,\*</sup>

5

6 <sup>1</sup> Department of Orthopaedic Surgery, University of California, San Diego, La Jolla, CA,  
7 USA

8 <sup>2</sup> Veterans Affairs San Diego Healthcare System, San Diego, CA, USA

9

10 \* Corresponding Author

11 Department of Orthopaedic Surgery

12 University of California, San Diego

13 9500 Gilman Drive, MC 0863

14 La Jolla, CA 92093

15 Tel.: 858-822-0720; Fax: (858) 822-3807

16 E-mail address: sbshah@ucsd.edu

17 *Keywords:* Peripheral nerve, Carpal tunnel syndrome, Cubital tunnel syndrome,  
18 decompression, biomechanics, rat

19 *This study was approved by our institution's IACUC.*

20 *Conflicts of Interest and Authors Contribution:* There are no conflicts of interest. All  
21 authors contributed to the acquisition, analysis, and interpretation of data. IF and SBS  
22 additionally contributed to the research design and manuscript writing. All authors edited  
23 the manuscript and approved the submitted version.

24 *Acknowledgements:* We gratefully appreciate support from the UCSD Academic Senate  
25 and United States Department of Veterans Affairs Award #IRX001471A.

1 **Abstract:**

2 Paraneurial adhesions have been implicated in the pathological progression of  
3 entrapment neuropathies. Surgical decompression of adhesions is often performed, with  
4 the intent of restoring nerve kinematics. The normal counterpart of adhesions, native  
5 paraneurium, is also thought to influence nerve deformation and mobility. However,  
6 influences of native or abnormal paraneurial structures on nerve kinematics have not  
7 been investigated. We measured regional strains in rat sciatic nerves before and  
8 immediately after decompression of native paraneurial tissue, and before and after  
9 decompression of abnormal paraneurial adhesions, which formed within 6 weeks of the  
10 initial decompression. Strain was significantly higher in the distal-femoral than the mid-  
11 femoral region of the nerve before either decompression. Decompression of native and  
12 abnormal paraneurial tissue removed this regional strain difference. Paraneurial tissues  
13 appear to play a major role in distributing peripheral nerve strain. Normal nerve strain  
14 distributions may be reconstituted following decompression, even in the presence of  
15 paraneurial adhesions.

16

17 **Introduction:**

18 Peripheral nerves are dynamic structures that must withstand significant mechanical  
19 forces while reliably conducting electrical impulses. Because nerves traverse  
20 articulating joints and frequently follow paths outside of the normal plane of joint motion,  
21 they stretch and glide during movement, while maintaining structural and functional  
22 integrity.(Topp and Boyd, 2006) Animal models have demonstrated that when nerves  
23 are subjected to prolonged or excessive strain above physiological thresholds, their  
24 electrical function is compromised.(Clark et al., 1992; Tanoue et al., 1996; Wall et al.,  
25 1992) In humans, excessive traction related to mechanical impingement is believed to  
26 contribute to the progression of entrapment neuropathies, such as carpal and cubital  
27 tunnel syndromes.(Mackinnon, 2002; Mahan et al., 2015; Ogata and Naito, 1986;  
28 Rempel et al., 1999; Tanoue et al., 1996)

29

30 Peripheral nerves are believed to have several adaptations to protect against excessive  
31 strain. One such protective mechanism, observed in both animal and human cadaveric  
32 models, is the increased compliance of nerves at joint regions compared with non-joint  
33 regions (Mason and Phillips, 2011; Phillips et al., 2004), to accommodate increased  
34 strains in the vicinity of articulating joints.(Boyd et al., 2005; Topp and Boyd, 2006;  
35 Wright et al., 2001; Wright et al., 1996) This heterogeneity in nerve compliance is  
36 observed in nerves both *in vivo* and *ex vivo*, and allows them to accommodate the  
37 increased physiologic strain associated with synovial joint motion without resulting in  
38 mechanical failure. The structural basis for this heterogeneous strain profile has not  
39 been fully elucidated. Mason and Phillips revealed that rat median nerves possess  
40 subtle differences in collagen fibril geometry between joint and non-joint regions,  
41 possibly explaining these biomechanical differences.(Mason and Phillips, 2011)  
42 However, the same study also indicated that such structural variance is not conserved  
43 across all nerves,(Mason and Phillips, 2011) suggesting the possibility of additional  
44 adaptations that regulate local compliance.

45

46 The paraneurium, also referred to as mesoneurium, is another possible modulator of  
47 local nerve compliance. It is composed of connective tissue that attaches the peripheral  
48 nerve to its surrounding nerve bed, and also carries the nerve's extrinsic segmental  
49 blood supply.(Lundborg, 1979) It has been hypothesized that that the paraneurium  
50 serves a mechanical function, guiding the trajectory of peripheral nerves within their  
51 beds and facilitating low-friction nerve "gliding".(Butler, 2000; Mazal and Millesi, 2005;  
52 Millesi et al., 1995; Smith, 1966) Moreover, the paraneurium has a pathologic  
53 counterpart frequently encountered in a surgical or other clinical setting:  
54 adhesions,(Millesi et al., 1993) which often describe abnormal connections between two  
55 tissue structures, such as two loops of bowel.(Smith, 1966) In peripheral entrapment  
56 neuropathies such as cubital tunnel syndrome, paraneurial adhesions are often  
57 implicated as causal agents of neural impingement and associated changes in traction,  
58 abnormally tethering the nerve to its surrounding structures.(Abe et al., 2005; Foran et  
59 al., 2016; Ochi et al., 2014; Topp and Boyd, 2006) Additionally, there is concern that  
60 adhesions eventually contribute to intraneural fibrosis, resulting in intraneural structural  
61 changes with deleterious mechanical and functional consequences(Ikeda et al., 2003;  
62 Yamamoto et al., 2010), as well as increased risk for recurrent entrapment (Botte et al.,  
63 1996; McCall et al., 2001; Steyers, 2002). The mainstay of surgical management of  
64 these syndromes often involves some form of neurolysis or decompression,(Foran et  
65 al., 2016; Millesi et al., 1993) with the intent of relieving mechanical effects of traction  
66 and entrapment on the nerve.

67 Despite empirical evidence supporting a mechanical role for the paraneurium, as well as  
68 a well-documented role for adhesions in the progression of entrapment neuropathy,  
69 influences of native or abnormal paraneurial tissue on peripheral nerve strain have not  
70 been examined. In this study we used a rat sciatic nerve model to investigate the effect  
71 of both normal paraneurial tissue and paraneurial adhesions, and the effect of surgical  
72 neurolysis of these tissues, on peripheral nerve strain.

73 **Methods:**

74 ***Rat surgeries and image analysis:***

75 All procedures were completed under protocols approved by our institutional IACUC.  
76 Twelve 10-week-old male Lewis rats (Harlan (now Envigo), Placentia, CA) were studied  
77 in this experiment. Rats were kept in standard group housing, 3 rats to a cage, with a  
78 normal diet and water. The rats were induced and maintained under anaesthesia at 10  
79 weeks of age with inhalational isoflurane delivered via nose cone. A 15 mm incision was  
80 made on the posterolateral thigh overlying the sciatic nerve with aseptic technique. The  
81 right or left sciatic nerve was chosen randomly for study by a random number generator  
82 (RANDOM.ORG). Using a gluteus splitting technique, the sciatic nerve was then  
83 carefully exposed using a combination of sharp and blunt dissection under a dissecting  
84 microscope from the level of the quadratus femoris muscle to the trifurcation of the  
85 tibial, common peroneal, and sural nerves. Care was taken not to disturb the  
86 paraneurial attachments of the nerve to the underlying nerve bed. Using a tissue  
87 marking pen, 5 epineurial markers were placed at about 4mm increments with the most  
88 proximal marker at the level of the quadratus femoris muscle and most distal marker at  
89 the level of the trifurcation (Figure 1). The region between the first and third marker was  
90 designated as “mid-femoral,” while the region between the third and fifth marker was  
91 defined as “distal-femoral.” A sterile ruler was placed into the wound to set scale, and  
92 pictures were then taken with the knee flexed to 90° and ankle maximally plantarflexed  
93 (relaxed configuration) and the knee extended to 0° and the ankle maximally dorsiflexed  
94 (stretched configuration). Next, the paraneurial connections from the level of the  
95 quadratus femoris to the trifurcation were sharply dissected with tenotomy scissors  
96 (decompression), with the knee in full flexion to minimize strain on the nerve during  
97 decompression. The knee and ankle were then placed into the two configurations above  
98 and pictures were again taken. The wound was then closed in layers with absorbable,  
99 braided 4-0 Vicryl suture (Ethicon, Somerville, NJ, USA).

100

101 Six weeks after the index surgery, rats were sacrificed with carbon dioxide and cervical  
102 dislocation, and the sciatic nerve was again exposed in the manner above under a

103 dissecting microscope. In all animals, adhesions were discovered connecting the sciatic  
104 nerve to the surrounding muscle, muscle fascia, fat, and nerve bed (Figure 1) in a  
105 distribution greater than the original native paraneurial tissues seen at week zero.  
106 Epineurial markers were placed as above using a tissue marking pen, at 4mm  
107 increments from the level of the quadratus femoris to the level of the trifurcation.  
108 Adhesive tissue was perforated, but not released, to access the underlying nerve for  
109 labeling. The knee and ankle were ranged through the same two joint configurations as  
110 above and pictures were taken. Next, the adhesions from the level of the quadratus  
111 femoris muscle to the trifurcation were sharply and fully dissected with scissors  
112 (decompression), freeing the nerve from all soft tissue connections in this region. The  
113 knee and ankle again were then placed into the two configurations above and pictures  
114 were taken. With all images obtained, nerves were harvested from just above the level  
115 of the quadratus femoris and just below the level of the trifurcation and placed into a  
116 freezer at -80° for future sectioning and analysis. Six sciatic nerves were also harvested  
117 from 10-week old Lewis rats to serve as controls. Contralateral controls were not used,  
118 due to the possibility of compensatory changes resulting from ipsilateral nerve damage.  
119 Images were analyzed using ImageJ (NIH) and strain was calculated based on marker-  
120 to-marker distances in the stretched position relative to the relaxed position. (Foran et  
121 al., 2016; Mahan et al., 2015) Edges of each ink dot in each joint configuration were  
122 used as fiducial markers, to improve accuracy of measurement. Average strain across  
123 the entire exposed region, maximum strain between any two adjacent markers, and  
124 regional nerve strain in the proximal and distal regions were calculated.

125

### 126 ***Nerve sectioning, trichrome, and immunohistochemistry***

127 All harvested nerves were thawed at -20°, embedded in Optimal Cutting Temperature  
128 compound, and flash frozen in liquid nitrogen cooled isopentane. Several 10 µm cross-  
129 sections were obtained using a cryostat (Leica CM 3050 S) proximally at the level of the  
130 first tissue marker (at the level of the quadratus femoris) and distally at the level of the  
131 fifth tissue marker (the level of the trifurcation). Sections were maintained in a freezer at  
132 -20° between sectioning and staining.

133

134 A proximal and distal section of each nerve underwent trichrome staining to allow for  
135 analysis of gross structural morphology and connective tissue content. Slides were  
136 thawed at room temperature for 15 minutes and then placed into neutral buffered  
137 formalin. They were then stained with Harris Modified Hemotoxylin (HHS128, Sigma-  
138 Aldrich, St. Louis, MO) for 4 minutes, followed by Gömöri's Trichrome Stain (#24205,  
139 Polysciences, Inc., Warrington, PA) for 5 minutes. Slides were then successively  
140 washed in acetic acid, alcohol, and citrisolv, and finally mounted with Permount  
141 medium.

142 A proximal and distal section of each nerve also underwent immunohistochemical  
143 staining for phosphorylated neurofilaments (SMI31; axonal marker) and laminin (basal  
144 lamina marker). Sections were fixed with 10% formalin, permeated with 0.2% Triton X-  
145 100, and blocked using a solution of 10% normal goat serum and 3% BSA in PBS. For  
146 laminin and neurofilament staining, sections were incubated with primary antibodies  
147 against laminin (1:500, Sigma Aldrich) and phosphorylated neurofilament (1:1000,  
148 SMI31, Sigma-Aldrich) for 1 hour at room temperature. After rinsing with PBS, sections  
149 were then incubated with Alexa Fluor-594 goat anti-mouse and Alexa-Fluor-488 goat  
150 anti rabbit (1:200, Life Technologies) for 1 hour at room temperature. Samples were  
151 imaged using a widefield fluorescence microscope (Leica DM 6000 B) to analyze  
152 neurofilament localization and the internal structure of the nerve.

153 Axon counts were performed using a semi-automated approach, from 63X images of  
154 SMI-31 labeled sections. Images were binarized using Image J (NIH), and axon  
155 densities calculated by summing axon numbers from three randomly selected regions of  
156 interest (ROI) within each section, and dividing by the summed area of these ROIs.

157 Axon counts were then estimated for the whole nerve by multiplying axon density by the  
158 intra-epineurial area of each section, measured from 20x images. Given the variability in  
159 attached extra-epineurial connective tissue following nerve excision, area-based  
160 measurements of connective tissue remodeling were unreliable. Therefore, trichrome  
161 images were scored semi-quantitatively to determine the integrity of the epineurium and  
162 the infiltration of adhesion tissue into the nerve. Blinded images and scoring criteria



163 were presented to 5 individuals with knowledge of basic nerve architecture, and images  
164 were scored based on a scale from 1 to 5. This scale reflects the circumferential extent  
165 of fusion between extra-epineurial tissue and the interior of the nerve, indicated by the  
166 loss of a clear external epineurial boundary (Table 1 and Figure 2). Sample images for  
167 each score were presented to individuals as training, prior to blind testing of the full set  
168 of images. Average scores from all 5 individuals for each image were used for statistical  
169 analysis.

170

### 171 ***Statistical analysis***

172 Average and maximum measured strains were compared using 2x2 two-way repeated  
173 measures ANOVA with factors of time (0 or 6 weeks) and surgical intervention (pre- or  
174 post-decompression). Proximal and distal strains were compared using 2x2 two-way  
175 repeated measures ANOVA with factors of surgical intervention (pre- or post-  
176 decompression) and region (proximal or distal), or factors of time point (0 or 6 weeks)  
177 and region (proximal or distal). Student's t-test was used to test for significant  
178 differences between epineurial integrity scores ( $\alpha = 0.05$ ). Data are given as Mean  
179 (SEM).

180 **Results:**

181 ***Nerve structure***

182 At week 0, prior to decompression, nerves were slack with neutral knee and ankle, but  
183 incurred tension upon knee extension and ankle dorsiflexion (Figure 1A-B). At week 6  
184 (42 days), the nerve trajectory in both neutral and stretched configurations was  
185 markedly altered, and overlying connective tissue was observed (Figure 1C-D). These  
186 changes did not appear to cause any apparent functional deficits, as assessed by toe-  
187 spreading. Gross vascular deficits were also not observed, based on minimal pooling of  
188 blood and a consistent coloration of nerves and visible regions of their targeted  
189 muscles. To investigate whether these extra-epineurial adaptations resulted in changes  
190 to the interior of the nerve, we performed immunohistochemistry. Blind scoring of tissue  
191 sections with trichrome labeling showed a significant decrease in epineurial integrity 6  
192 weeks after decompression, compared to controls (Figure 2). However,  
193 immunofluorescence labeling of axons (phosphorylated neurofilaments, red) and basal  
194 lamina (laminin, green) revealed that connective tissue infiltration into the interior of the  
195 treatment group nerves was not observed (i.e., internal epineurial borders remained  
196 sharp), and nerve fiber architecture appeared normal in both mid-femoral and distal-  
197 femoral regions of the nerve (Figure 3). Axon counts (0 weeks: 5324 (434); 6 weeks:  
198 5846 (312);  $p > 0.37$ ,  $n = 4$ ) and axonal density (0 weeks:  $9.9 \times 10^{-3}$  ( $2.6 \times 10^{-4}$ ); 6 weeks:  
199  $9.8 \times 10^{-3}$  ( $6.0 \times 10^{-4}$ );  $p > 0.92$ ,  $n = 4$ ) were not significantly different.

200

201 ***Nerve Strain***

202 Average and maximum sciatic nerve strains were measured before and after  
203 decompression, at 0 and 6 weeks. Average strains (Mean $\pm$ SEM) prior to  
204 decompression at week 0 and week 6 were 17.64% (4.5%) and 16.17% (2.14%),  
205 respectively. Average strains after decompression at week 0 and week 6 were 18.5%  
206 (3.35%) and 17.49% (4.5%), respectively. Maximum strains prior to decompression at  
207 week 0 and week 6 were 32.14% (6.35%) and 31.28% (3.9%), respectively. Maximum  
208 strains after decompression at week 0 and week 6 were 28.80% (4.15%) and 31.73%  
209 (5.02%), respectively. No significant differences were observed in either average or

210 maximum strains before and after decompression at either time point. We did, however,  
211 observe significant regional differences in sciatic nerve strain (Figure 4). At 0 weeks,  
212 strain in the distal-femoral region (i.e., just proximal to the trifurcation) was significantly  
213 higher than that in the mid-femoral region (23.91% (5.4%) vs. 12.41% (4.07%),  
214  $P < 0.001$ ) prior to decompression, but this regional strain difference disappeared after  
215 decompression (Figure 4A). Similarly, prior to decompression at 6 weeks, nerve strain  
216 in the distal-femoral region was significantly higher than that in the mid-femoral region  
217 (20.51% (3.86%) vs. 12.26% (2.23%),  $P < 0.05$ ); again, this regional strain difference was  
218 not observed after decompression (Figure 4B).

219 **Discussion:**

220 Several studies have suggested a mechanical role for the paraneurium, in guiding nerve  
221 trajectory and in enabling controlled nerve gliding within its bed.(Butler, 2000; Mazal and  
222 Millesi, 2005; Millesi et al., 1995; Smith, 1966) Additionally, in an early investigation of  
223 peripheral nerve blood supply, Smith observed that nerves *in situ* displayed greater  
224 elasticity than those removed from their “mesoneurial” attachments.(Smith, 1966) He  
225 noted, “The fact that an isolated nerve has far less capacity for stretching than one in  
226 situ suggests that it is mainly the mesoneurium which allows for adjustments in length of  
227 the nerve.” Later, Millesi also described the apparent mechanical importance of the  
228 structure he termed the “paraneurium.” He noted that this structure appeared to be  
229 designed to allow for nerve motion and caliber changes. He also recognized that the  
230 paraneurium could become fibrotic, forming adhesions: “shrinkage of the fibrotic  
231 paraneurium... may cause compression of the entire nerve trunk, like a stocking that is  
232 too tight.”(Millesi et al., 1995) Although these investigators inductively reasoned that the  
233 paraneurium might modulate tensile nerve mechanics based upon gross observation,  
234 the nature of such a role remained to be tested.

235

236 In this study, we found that both normal paraneurium and its abnormal counterpart,  
237 adhesions, significantly impacted the distribution of strain in rat sciatic nerves. When  
238 normal paraneurial tissues were intact, regional differences in strain were observed,  
239 with increased strain in the distal-femoral region of the nerve compared to mid-femoral  
240 regions. Strikingly, an almost-identical strain gradient was recreated within 6 weeks  
241 after the initial decompression, in spite of differences in the trajectory of the nerve within  
242 its bed. This gradient was again eliminated the adhesion tissue was decompressed. The  
243 elimination of regional differences in strain by surgical decompression indicates that  
244 paraneurial attachments play an essential role in directing strain along the course of  
245 nerves. The underlying rationale for relative compliance of the more distal region of the  
246 nerve is not completely clear, but may result from proximity to the articulating knee joint  
247 (cf. (Boyd et al., 2005; Wright et al., 2001; Wright et al., 1996)), compliance required for  
248 trajectory changes of a trifurcation, or both.

249 Our data have several important clinical implications. The first is that surgeries that  
250 divide paraneurium or adhesions may have unpredictable consequences. Peripheral  
251 nerves are frequently dissected free of their paraneurial attachments during surgery,  
252 either to mobilize them for purposes of exposure, or during decompression procedures.  
253 However, releasing these nerves from their paraneurial tissues for purposes of  
254 mobilization may redistribute strain along the nerve, as recently described for the ulnar  
255 nerve, following its release during surgical treatment of cubital tunnel syndrome.(Foran  
256 et al., 2016) More persistent redistribution of strain from nerve regions accustomed to  
257 high strain to less compliant regions of the nerve may alter nerve susceptibility to  
258 structural and functional injury. It is not unreasonable to posit that neuropraxia and  
259 nerve injuries of greater severity, which are commonplace after these exposures, may  
260 be a result of altered mechanical loading subsequent to neurolysis, rather than a direct  
261 mechanical insult from retractors.(McConaghie et al., 2014)

262 Also compelling is our discovery that adhesion tissue appears to reconstitute strain  
263 distributions seen in control nerves, in both orientation and magnitude. This finding  
264 raises the possibility that the seemingly “random” generation of fibrous tissue exhibited  
265 by adhesions may instead participate in or respond to an organized process that  
266 attempts to recreate the normal neural biomechanical environment. This raises the  
267 question of whether the formation of adhesion tissue is necessarily pathological.  
268 Several strategies have been proposed to limit formation of adhesion tissue. However,  
269 rarely is consideration given as to whether paraneurial structures – whether native  
270 paraneurium or adhesions – may in some cases represent a positive biological  
271 response, possibly in response to mechanical loads experienced, and perhaps even  
272 favored, by peripheral nerves.(Anava et al., 2009; Pfister et al., 2004; Simpson et al.,  
273 2013) It is worth noting that rats were not immobilized in this study. It may be that  
274 immobilization, which is frequently recommended to patients following surgery or  
275 traumatic injury, leads to an absence of mechanical stimuli, driving the formation of a  
276 pathologic tether. Further research comparing nerve kinematics in the context of  
277 adhesion formation with and without immobilization will be needed to investigate this  
278 possibility.

279 An interesting methodological note is that paraneurial adhesion formation in our study  
280 required little more than incision, dissection of the paraneurial structures about the  
281 nerve, closure with absorbable braided sutures, and the passage of time. Gross  
282 observations of fibrotic tissue, as well as histological findings indicating a loss of  
283 epineurial integrity, confirm the formation of adhesions, despite use of reproducible and  
284 conservative surgical technique. Similar phenotypes have also been previously reported  
285 by Millesi, as indicators of adhesion formation.(Mazal and Millesi, 2005; Millesi et al.,  
286 1995) The ease of forming adhesion tissue is of interest, as a prior study reported the  
287 formation of adhesions in the sciatic nerves of rabbits by both cauterization of the nerve  
288 bed as well as suturing of the nerve to the surrounding nerve bed, followed by 5-6  
289 weeks passage of time.(Abe et al., 2005) This latter method of forming adhesions is  
290 problematic for study purposes involving biomechanics, as suturing of the nerve to the  
291 nerve bed in and of itself results in a mechanical tether that affects future strain  
292 measurements.(Mahan et al., 2015) Our method of producing adhesions is highly  
293 reproducible and does not require nerve suturing, which may be helpful to other  
294 investigators in future studies.

295 Our study has several limitations. We measured nerve surface (epineurial) strain by  
296 measuring displacement of epineurial markings, rather than directly measuring strain  
297 with a microstrain gauge or other method. Despite the comparatively low resolution of  
298 our approach, we avoided damage to the neural elements, and our nerve strain findings  
299 were in keeping with prior studies.(Topp and Boyd, 2006) We also did not measure  
300 nerve strain distal or proximal to the exposed region of the sciatic nerve. It is possible  
301 that nerve strain following paraneurial decompression was transferred somewhere  
302 along the course of an unexposed region of the nerve. Further investigations will be  
303 needed to quantify this possibility, and would be aided by the development of  
304 noninvasive approaches to imaging less accessible nerve regions. Additionally, while  
305 we did not observe any pooling of blood or change in tissue coloration indicative of overt  
306 ischemia, more investigation is needed to determine the functional effects of paraneurial  
307 decompression on neural electrical conduction and blood flow. A final limitation is the  
308 nature of adhesions that were created following surgical decompression of otherwise  
309 healthy tissue. Such adhesions likely more closely resemble those formed following

310 surgical dissection than those formed following injury or during neuropathic progression.  
311 Such conditions may result in damage to nerve fibers, an altered inflammatory  
312 environment, and fibrosis, all of which could impact resultant mechanical sequelae.

313 **References:**

- 314 Abe Y, Doi K, Kawai S. An experimental model of peripheral nerve adhesion in rabbits.  
315 Br J Plast Surg. 2005, 58: 533-40.
- 316 Anava S, Greenbaum A, Ben Jacob E, Hanein Y, Ayali A. The regulative role of neurite  
317 mechanical tension in network development. Biophys J. 2009, 96: 1661-70.
- 318 Botte MJ, von Schroeder HP, Abrams RA, Gellman H. Recurrent carpal tunnel  
319 syndrome. Hand Clin. 1996, 12: 731-43.
- 320 Boyd BS, Puttlitz C, Gan J, Topp KS. Strain and excursion in the rat sciatic nerve during  
321 a modified straight leg raise are altered after traumatic nerve injury. J Orthop Res. 2005,  
322 23: 764-70.
- 323 Butler DS. *The sensitive nervous system*, 1st edn. Adelaide, Noigroup Publications,  
324 2000.
- 325 Clark WL, Trumble TE, Swiontkowski MF, Tencer AF. Nerve tension and blood flow in a  
326 rat model of immediate and delayed repairs. J Hand Surg Am. 1992, 17: 677-87.
- 327 Foran I, Vaz K, Sikora-Klak J, Ward SR, Hentzen ER, Shah SB. Regional ulnar nerve  
328 strain following decompression and anterior subcutaneous transposition in patients with  
329 cubital tunnel syndrome. J Hand Surg Am. 2016, 41: e343-e50.
- 330 Ikeda K, Yamauchi D, Osamura N, Hagiwara N, Tomita K. Hyaluronic acid prevents  
331 peripheral nerve adhesion. Br J Plast Surg. 2003, 56: 342-7.
- 332 Lundborg G. The intrinsic vascularization of human peripheral nerves: Structural and  
333 functional aspects. J Hand Surg Am. 1979, 4: 34-41.
- 334 Mackinnon SE. Pathophysiology of nerve compression. Hand Clin. 2002, 18: 231-41.
- 335 Mahan MA, Vaz KM, Weingarten D, Brown JM, Shah SB. Altered ulnar nerve kinematic  
336 behavior in a cadaver model of entrapment. Neurosurgery. 2015, 76: 747-55.
- 337 Mason S, Phillips JB. An ultrastructural and biochemical analysis of collagen in rat  
338 peripheral nerves: The relationship between fibril diameter and mechanical properties. J  
339 Peripher Nerv Syst. 2011, 16: 261-9.
- 340 Mazal PR, Millesi H. Neurolysis: Is it beneficial or harmful? Acta Neurochir Suppl. 2005,  
341 92: 3-6.



342 McCall TD, Grant GA, Britz GW, Goodkin R, Kliot M. Treatment of recurrent peripheral  
343 nerve entrapment problems: Role of scar formation and its possible treatment.  
344 Neurosurg Clin N Am. 2001, 12: 329-39.

345 McConaghie FA, Payne AP, Kinninmonth AW. The role of retraction in direct nerve  
346 injury in total hip replacement: An anatomical study. Bone Joint Res. 2014, 3: 212-6.

347 Millesi H, Rath T, Reihsner R, Zoch G. Microsurgical neurolysis: Its anatomical and  
348 physiological basis and its classification. Microsurgery. 1993, 14: 430-9.

349 Millesi H, Zoch G, Reihsner R. Mechanical properties of peripheral nerves. Clin Orthop  
350 Relat Res. 1995: 76-83.

351 Ochi K, Horiuchi Y, Nakamura T, Sato K, Morita K, Horiuchi K. Associations between  
352 ulnar nerve strain and accompanying conditions in patients with cubital tunnel syndrome.  
353 Hand Surg. 2014, 19: 329-33.

354 Ogata K, Naito M. Blood flow of peripheral nerve effects of dissection, stretching and  
355 compression. J Hand Surg Br. 1986, 11: 10-4.

356 Pfister BJ, Iwata A, Meaney DF, Smith DH. Extreme stretch growth of integrated axons.  
357 J Neurosci. 2004, 24: 7978-83.

358 Phillips JB, Smit X, De Zoysa N, Afoke A, Brown RA. Peripheral nerves in the rat exhibit  
359 localized heterogeneity of tensile properties during limb movement. J Physiol. 2004,  
360 557: 879-87.

361 Rempel D, Dahlin L, Lundborg G. Pathophysiology of nerve compression syndromes:  
362 Response of peripheral nerves to loading. J Bone Joint Surg Am. 1999, 81: 1600-10.

363 Simpson AH, Gillingwater TH, Anderson H et al. Effect of limb lengthening on internodal  
364 length and conduction velocity of peripheral nerve. J Neurosci. 2013, 33: 4536-9.

365 Smith JW. Factors influencing nerve repair. II. Collateral circulation of peripheral nerves.  
366 Arch Surg. 1966, 93: 433-7.

367 Steyers CM. Recurrent carpal tunnel syndrome. Hand Clin. 2002, 18: 339-45.

368 Tanoue M, Yamaga M, Ide J, Takagi K. Acute stretching of peripheral nerves inhibits  
369 retrograde axonal transport. J Hand Surg Br. 1996, 21: 358-63.

370 Topp KS, Boyd BS. Structure and biomechanics of peripheral nerves: Nerve responses  
371 to physical stresses and implications for physical therapist practice. Phys Ther. 2006,  
372 86: 92-109.

373 Wall EJ, Massie JB, Kwan MK, Rydevik BL, Myers RR, Garfin SR. Experimental stretch  
374 neuropathy. Changes in nerve conduction under tension. J Bone Joint Surg Br. 1992,  
375 74: 126-9.

376 Wright TW, Glowczewskie F, Jr., Cowin D, Wheeler DL. Ulnar nerve excursion and  
377 strain at the elbow and wrist associated with upper extremity motion. J Hand Surg Am.  
378 2001, 26: 655-62.

379 Wright TW, Glowczewskie F, Wheeler D, Miller G, Cowin D. Excursion and strain of the  
380 median nerve. J Bone Joint Surg Am. 1996, 78: 1897-903.

381 Yamamoto M, Endo N, Ito M et al. Novel polysaccharide-derived hydrogel prevents  
382 perineural adhesions in a rat model of sciatic nerve adhesion. J Orthop Res. 2010, 28:  
383 284-8.

384

385 **Table Legend:**

Score	Criterion
1	Complete extracellular tissue infiltration through the epineurium and into the nerve.
2	An amount of extracellular tissue fusion with the epineurium greater than or equal to 50% of the circumference of the nerve.
3	An amount of extracellular tissue fusion with the epineurium greater than or equal to 20% but less than 50% of the circumference of the nerve.
4	An amount of extracellular tissue fusion with the epineurium less than 20% of the circumference of the nerve.
5	Complete absence of extracellular tissue fusion with the epineurium.

386

387 Table 1. Criteria for assigning Epineurial Integrity Scores, based on trichrome labeling.

388 Sample images for each score are shown in Figure 2. A score of 1 was not recorded for

389 any sections.

390 **Figures**

391 Figure 1. Macroscopic view of nerve trajectories just prior to the initial decompression  
392 (A-B, Day 0) and 6 weeks after the initial decompression, but before a second  
393 decompression (C-D, Day 42). (A) Nerve trajectory in a relaxed position at Day 0 (hip  
394 abducted, knee flexed 90°, ankle neutral). Also indicated on this image are sample  
395 epineurial markings used to make strain measurements. Exposed nerve was divided  
396 into two regions, mid-femoral and distal-femoral, for regional strain analysis. Ruler is  
397 demarcated in mm. (B) Nerve trajectory in a joint configuration inducing strain at Day 0  
398 (hip abducted, knee fully extended (180°), ankle maximally dorsi-flexed). (C) Nerve  
399 trajectory in a relaxed position at Day 42 (hip abducted, knee flexed 90°, ankle neutral).  
400 (D) Nerve trajectory in a joint configuration inducing strain at Day 42 (hip abducted,  
401 knee fully extended (180°), ankle maximally dorsi-flexed).

402

403 Figure 2. Trichome labeling was used to assess epineurial integrity 42 days after  
404 decompression for sham operated and decompressed nerves. (A-D) Sample images of  
405 completely intact (Score 5, A) to largely disrupted (Score 2, D) epineurium, with images  
406 shown from each experimental group. Scale bars are 200µm. Epineurial integrity scores  
407 were assessed based on criteria provided in Table 1. No tissue sections were scored  
408 with “Score 1” in either experimental group. (E) Comparison of semi-quantitative scoring  
409 of epineurial integrity reveals decreased integrity after decompression.

410

411 Figure 3. Phospho-neurofilament/laminin staining of mid-femoral and distal-femoral  
412 regions of nerve cross-sections from sham operated (A-B) and decompressed (C-D)  
413 nerves show intact axonal and intra-epineurial structure in both experimental groups.  
414 Axons are indicated by phosphorylated neurofilaments (red), and basal lamina is  
415 indicated by laminin (green). Insets are shown below the full cross-sectional image.  
416 Scale bars are 100µm.

417

418 Figure 4. Regional rat sciatic nerve strains before and after the initial decompression (A,  
419 Day 0) and before and after a second decompression 6 weeks after the initial  
420 decompression (B, Day 42). Distal strain is significantly higher than proximal strain  
421 ( $P < 0.001$ ) prior to decompression at both time points. 2-way repeated measures  
422 ANOVA revealed an interaction effect of region and decompression on strain at Day 0  
423 ( $p < 0.027$ ) and an effect of decompression on strain at Day 42 ( $p < 0.05$ ). Asterisks  
424 indicate significant differences between individual groups based on post-hoc testing.

425

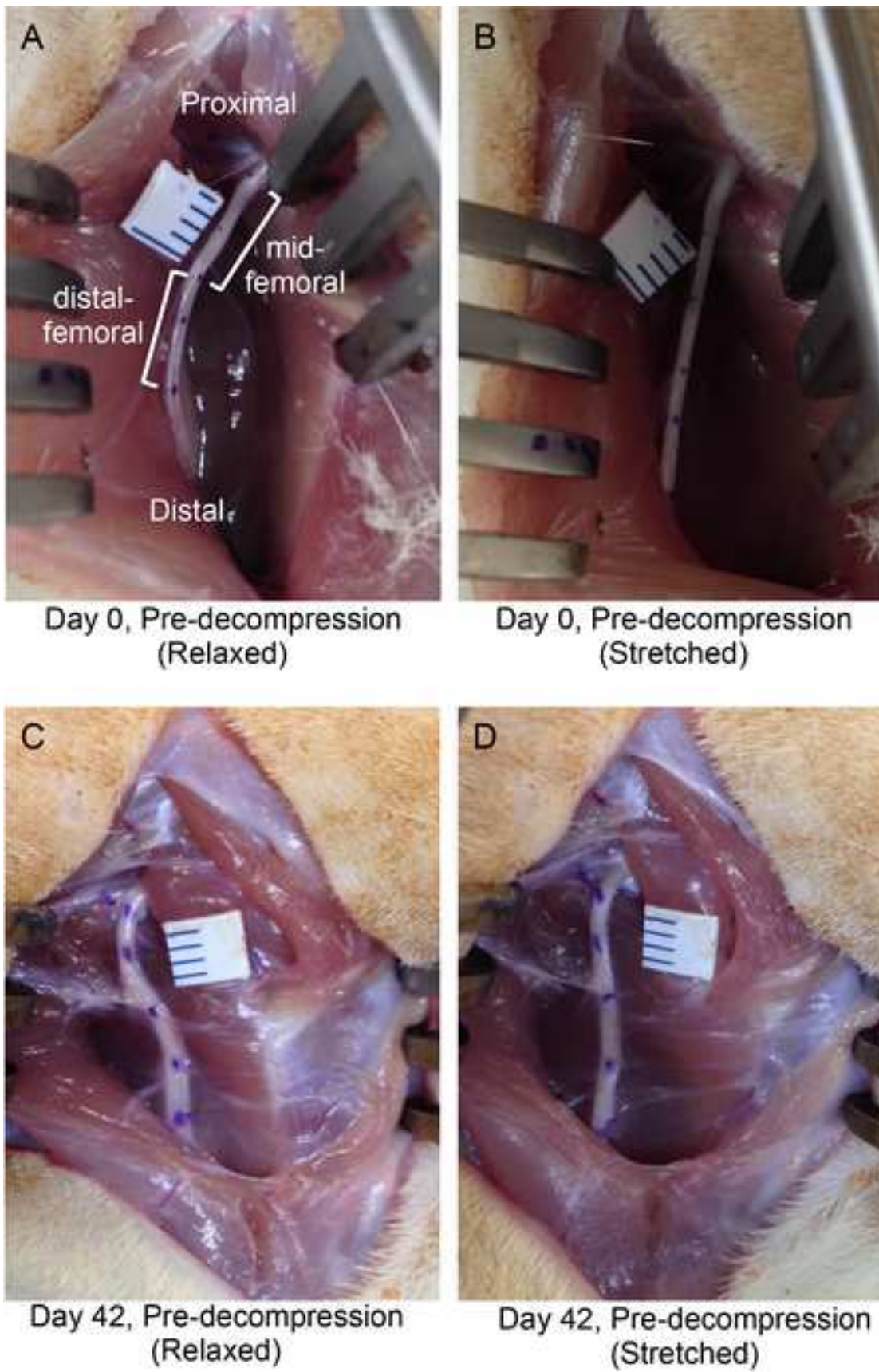


Figure 1

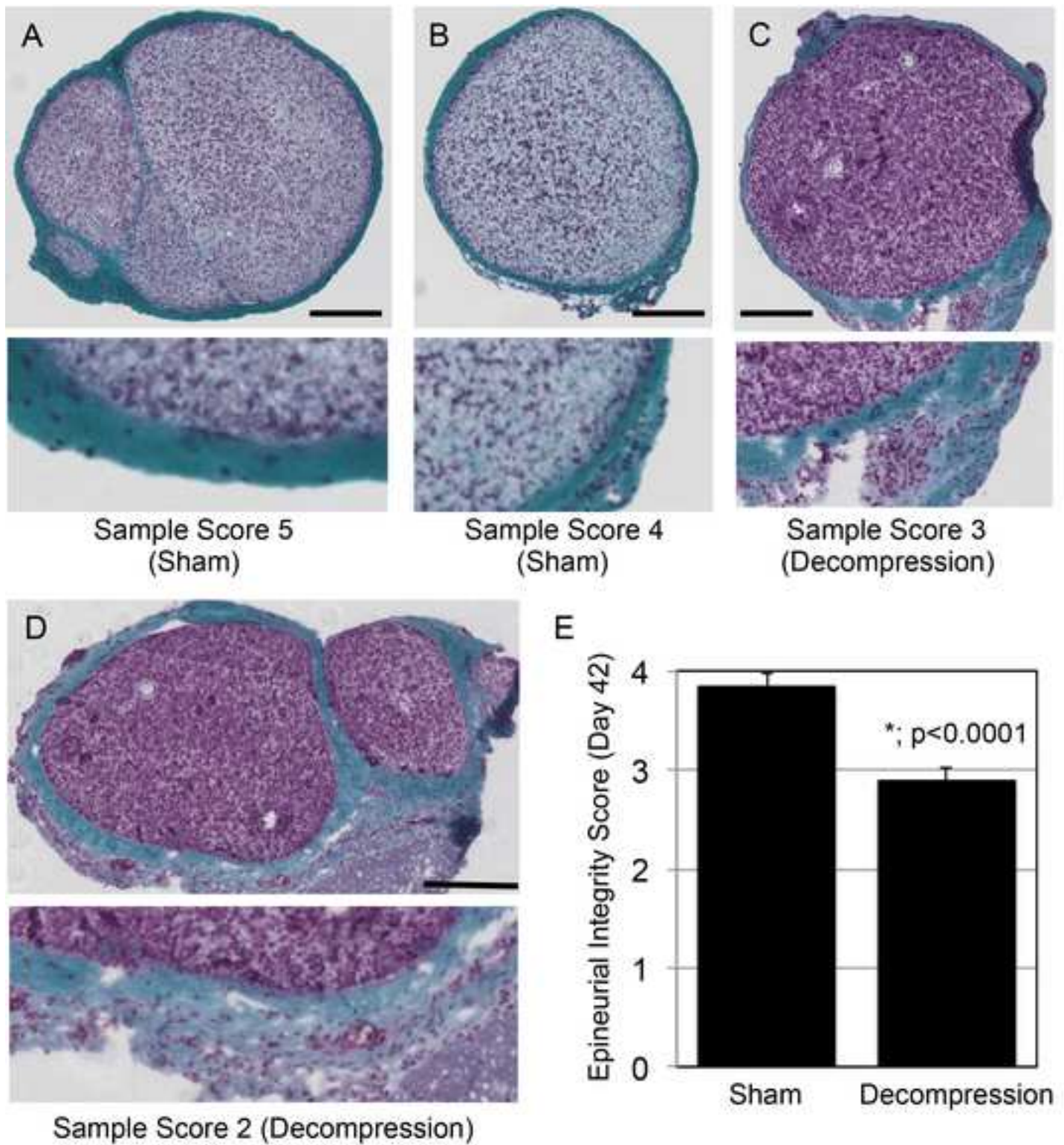


Figure 2

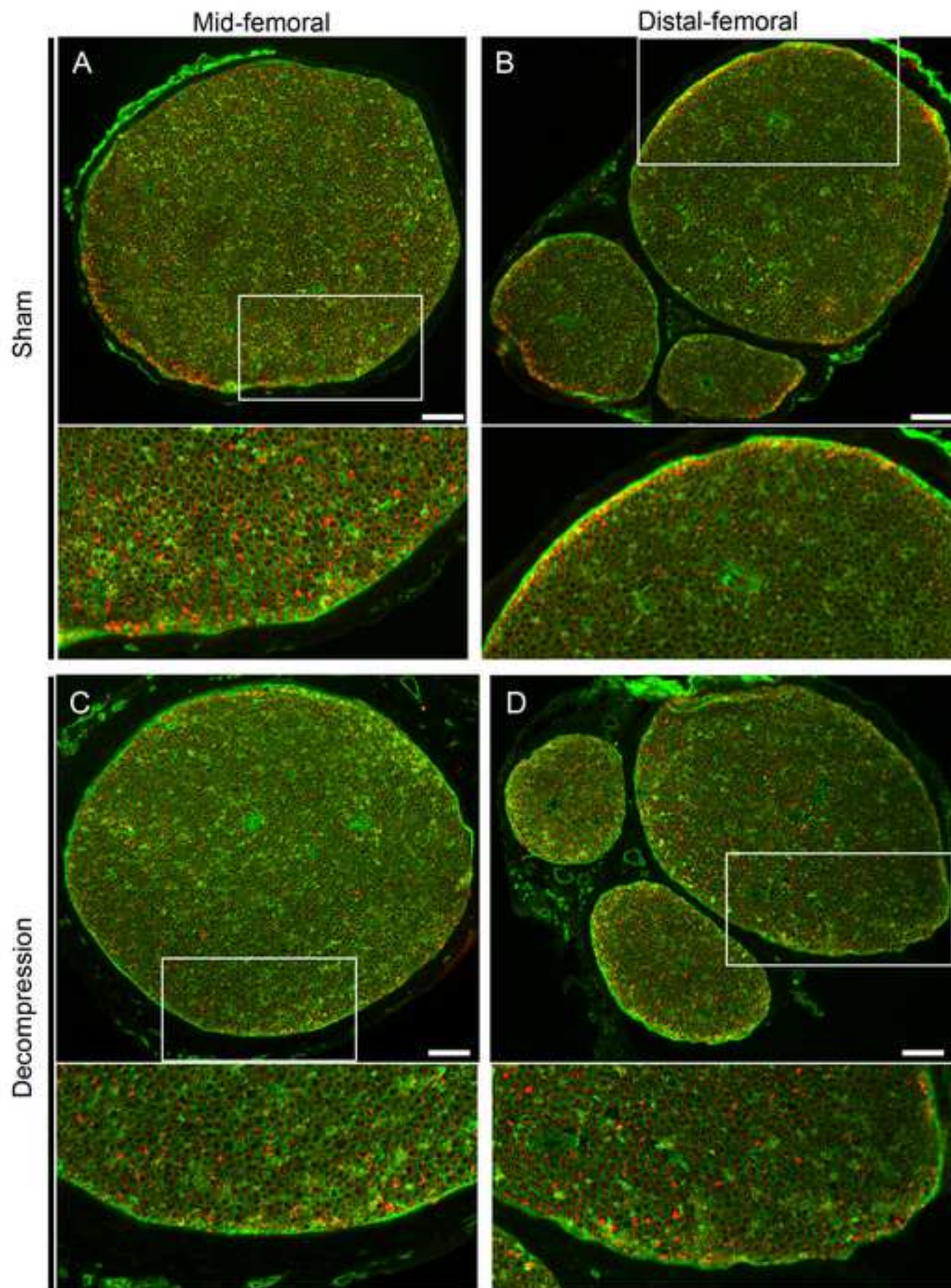


Figure 3



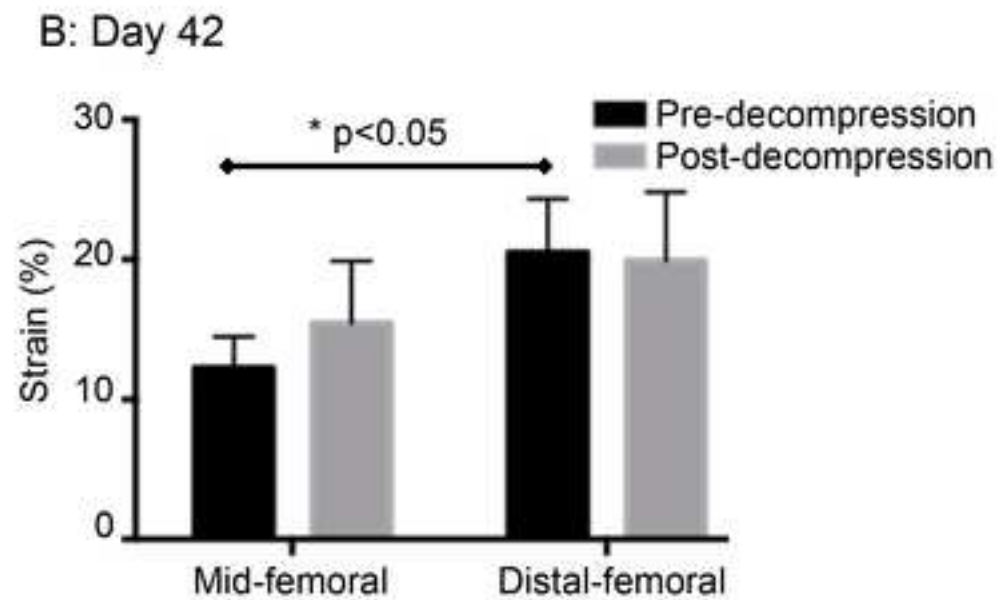
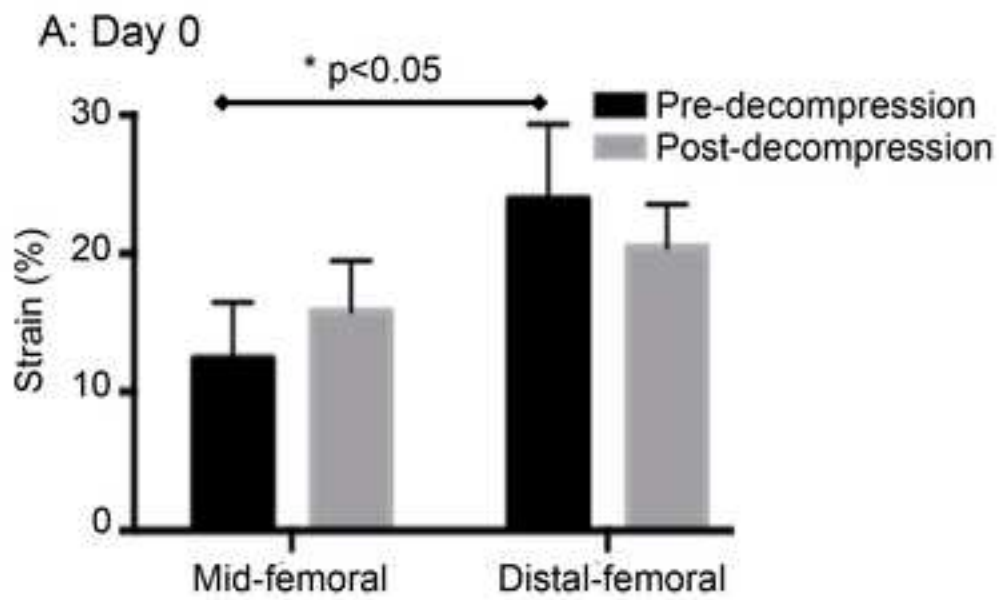


Figure 4